
A model of the role of adaptation and disadaptation in olfactory receptor neurons: implications for the coding of temporal and intensity patterns in odor signals

Paul A. Moore

Monell Chemical Senses Center, 3500 Market Street, Philadelphia,
PA 19104-3308, USA

Abstract. Natural odors occur as turbulent plumes resulting in spatially and temporally variable odor signals at the chemoreceptor cells. Concentrations can fluctuate widely within discrete packets of odor and individual packets are very intermittent and unpredictable. Chemoreceptor cells display the temporally dynamic properties of adaptation and disadaptation, which serve to alter their responses to these fluctuating odor patterns. A computational model, modified from one previously published, was used to investigate the effect of adaptation and recovery of adaptation (disadaptation) on the spike output of model olfactory receptor cells under natural stimulus conditions. The response characteristics of model cells were based upon empirically determined dose–response, adaptation, disadaptation and flicker fusion properties of peripheral olfactory cells. The physiological properties of the model cell (adaptation and disadaptation rate and the dose–response relationship) could be modified independently, allowing assessment of the role of each in shaping the responses of the model cell. Complete adaptation and disadaptation time courses ranged from 500 ms (rapid cells) to 10 s (slow cells). The stimuli for the model cells were quantified odor plume recordings obtained under a variety of biologically relevant flow conditions. As expected, the rapidly adapting model cells displayed different response characteristics than the slowly adapting model cells to identical temporal odor profiles. Responses of the model cells depended upon their adaptation and disadaptation rates, and the frequency characteristics of the odor presentation. These results indicate that adaptation and disadaptation determine the range of concentration fluctuations over which a particular cell will respond. Thus, these properties function as an olfactory equivalent of a band-pass filter in electronics. This type of filtering has implications for the extraction of information from odor signals, such as the coding of temporal and intensity features.

Introduction

The physiological responses of chemoreceptor cells often return to pre-stimulus levels in spite of continual stimulation. This process, termed adaptation, can be thought of as a dynamic change in the response threshold of the receptor cell (Kaissling *et al.*, 1987; Borroni and Atema, 1988). Under constant stimulation, adaptation will cause the response threshold of the cell to rise to the level of the stimulus, thus decreasing the firing rate of the receptor cell. Conversely, recovery from adaptation, here termed disadaptation, is the lowering of the response threshold from the removal of the stimulus or a decrease in the stimulus concentration. After a period of no stimulation, the receptor cell's threshold will return to its original level (Voigt and Atema, 1990). Together, adaptation and disadaptation serve a functional role as a temporal filter for chemoreceptor cells (Moore and Atema, 1988).

Physiological studies of the temporal response properties of invertebrate chemoreceptors have focused on pulse frequency resolution (Kaissling *et al.*, 1987; Christensen and Hildebrand, 1988; Rumbo and Kaissling, 1989; Almaas *et al.*, 1991; Gomez *et al.*, 1992), adaptation and disadaptation rates (Voigt and Atema, 1990), dynamic changes in receptor threshold (Borroni and Atema, 1988), and changes in generator potential (Michel and Ache, 1991). These properties arise in part from different

physio-chemical processes within a chemoreceptor cell, such as receptor phosphorylation and changes in Ca^{2+} stores. Individually, these studies have provided insight into how chemoreceptor cells adapt, and over what time frame adaptation and disadaptation occurs. It is only when these studies are coupled with knowledge of natural stimulus patterns that the functional role of adaptation as a temporal filter for odor information becomes apparent.

To characterize the different aspects of adaptation and disadaptation, previous studies have concentrated on stimulus presentations that were not representative of the stimulus profiles found in natural environments (Kaissling *et al.*, 1987; Borroni and Atema, 1988; Voigt and Atema, 1990). This resulted from either a lack of detailed knowledge of the natural structure of odor signals in environment or the inability to deliver identical turbulent odor profiles to different cells during electrophysiological recording. To fully characterize the roles that adaptation and disadaptation perform in filtering of chemical signals, a two-fold experiment must be performed. First, the adaptation and disadaptation rates of multiple receptor cells must be determined with static pulses. Then, these cells must be presented with quantified turbulent odor signals. Technical difficulties in the measurement and controlled delivery of biologically relevant odor signals have made the latter experiment difficult.

The fine-scale structure of chemical signals, at biologically relevant time and space scales, is spatially and temporally heterogeneous and chaotic (Murlis and Jones, 1981; Murlis *et al.*, 1991; Atema, 1988; Moore and Atema, 1991; Moore *et al.*, 1994). Chemical signals arrive at receptor organs as discrete packets that vary in intensity and duration (Murlis and Jones, 1981; Moore and Atema, 1991). Odor concentrations can fluctuate widely within bursts and individual bursts are intermittent and unpredictable. Near the odor source, concentration fluctuations are large and the frequencies in the signal are the highest. As the odor signal travels away from the source, signal frequencies become lower, concentration fluctuations are smaller and periods of little or no signal become more frequent. Spatial and temporal changes in the signal structure occur with distance from the odor source.

Both terrestrial and aquatic animals use odor signals to make directional choices that are necessary to locate food, shelters and mates (Bell and Tobin, 1982; Kennedy, 1986; Johnsen and Teeter, 1980; Hodgeson and Mathewson, 1972). These animals must extract directional or distance information from the chaotic structure of the odor signal to orient effectively within odor plumes. The intermittent structure of these signals is necessary for some animals to sustain upwind movement within odor plumes (Cardé *et al.*, 1984). Thus, the temporal filter properties of chemoreceptor cells seem to play an important role in the coding of dynamic chemical signals and the extraction of information from odor plumes.

The purpose of this study was to investigate the effect that different rates of adaptation and disadaptation have on the responses of olfactory receptor cells under realistic environmental stimulus conditions. The ideal approach to investigating this problem would be to determine the adaptation and disadaptation properties of single cells within a population, and then stimulate them with identical turbulent odor presentations. Unfortunately, the fine-scale measurement and control of turbulent stimulus profiles within stimulus chambers is not possible. Thus, a computational model of chemoreceptor cells with adaptation and disadaptation properties can serve to provide insight into the coding

of stimulus profiles where electrophysiological techniques are inadequate. This model is an expansion of a previously published chemoreceptor model that dealt exclusively on disadaptation (Moore and Atema, 1988), and incorporates adaptation, disadaptation and dose–response properties. This model is not designed to address questions about the cellular processes of adaptation or disadaptation, but rather deals only with the functional significance of adaptation and disadaptation for the extraction of information from realistic environmental odor signals.

The stimuli for the computer model are odor profiles measured under turbulent conditions within a laboratory flume (Moore and Atema, 1991). These signals were recorded under the same flow conditions in which lobsters, *Homarus americanus*, orientated to an odor source. Thus, they have a real basis of providing spatial information during chemosensory orientation. In addition, they were sampled at the same spatial and temporal scales over which lobster chemoreceptors junction. To match the spatial sampling area associated with a single sensillum, electrochemical electrodes with diameters of 100–150 μm were used. Neurons in moths can respond to odor pulses as rapid as 10 Hz (Kaissling *et al.*, 1987; Christensen and Hildebrand, 1988; Rumbo and Kaissling, 1989) and peripheral chemoreceptor cells in lobsters can follow 4 Hz pulses of odors (Gomez *et al.*, 1992). These studies indicate that temporal sampling rates are between 100 and 500 ms. Thus, a sampling rate of 10 Hz in an aquatic medium should give a biologically realistic resolution of odor plumes.

Materials and methods

Receptor model

The receptor model was based on results from self-adaptation experiments (adaptation to the same compounds) and does not include the phenomenon of cross-adaptation (adaptation to different compounds). Some of the basic assumptions about receptor cell physiology and disadaptation were taken from a previously published model that dealt exclusively with disadaptation (Moore and Atema, 1988). Behavioral (Cain, 1970; Berglund *et al.*, 1971; Todrank *et al.*, 1991) and electrophysiology (Zack-Strausfeld and Kaissling, 1986; Borroni and Atema, 1988; Voigt and Atema, 1990; Borroni and O'Connell, 1992) studies have shown that, at least in some animals, self-adaptation causes shifts in dose–response functions of receptor cells. Thus, at any instant, response threshold is a function of the adaptation state of the receptor cell. The response threshold is determined by two independent processes; adaptation and disadaptation; which are time (t) and concentration (C) dependent.

Previously encountered concentrations of a stimulus will have cumulative, time-dependent effects on the threshold of the receptor cell. The total time (T) over which a sampled concentration will affect the threshold of a model cell is divided into adaptation (T_a) and disadaptation (T_d). T_a and T_d range from 0.1 to 40 s for complete adaptation or disadaptation in lobster olfactory cells (Voigt and Atema, 1990), but seem to be faster for insect olfactory cells (Kaissling, 1985; Kaissling *et al.*, 1987; Christensen and Hildebrand, 1988; Bartell and Rumbo, 1985), and similar for salamander olfactory cells (Baylin and Moulton, 1979). For the purposes of this study, T_a and T_d can range between 0.5 and 10 s. The magnitude of these effects depends on the magnitude of the previously sampled concentration (C) and the time since their occurrence (t).

The effect that a previous concentration has on the threshold of the model cell increases exponentially with time until the end of T_a and then decreases exponentially with time until the end of T_d (Figure 1). Equation 1 was used to generate the weight function (W_{T_a}) for the adaptation phase (T_a in Figure 1) and equation 2 was used for the weight function (W_{T_d}) for the disadaptation phase (T_d in Figure 1) over the previous sample period (T). Separate equations were used for adaptation and disadaptation so T_a and T_d could vary independently of each other.

$$W_{T_a} = 0.55 \times 1.5^{(0.1 \times t)} / \sum W_{T_a} \text{ for all values } t = 0 \text{ to end of } T_a \quad (1)$$

$$W_{T_d} = 0.55 \times 1.5^{(0.1 \times (T-t))} / \sum W_{T_d} \text{ for all values } t = T_a \text{ to } T \quad (2)$$

The values 1.5 and 0.1 were chosen to scale rise and decay of the weight function for the time periods between 0.5 and 10 s. Dividing the weight function by the sum and multiplying by 0.55 serves three purposes. First, T_a and T_d can vary independently of each other and the model will stay stable. Secondly, when the stimulus concentration is constant and the model has reached equilibrium, the model cell threshold is constant. Finally, under these conditions the model cell threshold is set at 10% above the stimulus concentration. This keeps a constant Weber fraction (Weber, 1978) of 10% for the response of the model cell irrespective of the stimulus concentration. This value (10%) is a little conservative as compared to those reported for animal behavior (2–33%), including humans (Cain, 1977a, b; McBurney *et al.*, 1967; Zimmer-Faust, 1991; catfish reference). Under these assumptions, the model cell threshold (R_t) at any time is given by equation 3:

$$R_t = \sum C_t \times W_t \text{ for values } t = T \text{ to } 0 \quad (3)$$

where C_t is the stimulus concentration at time t and W_t is the weight function W_a or

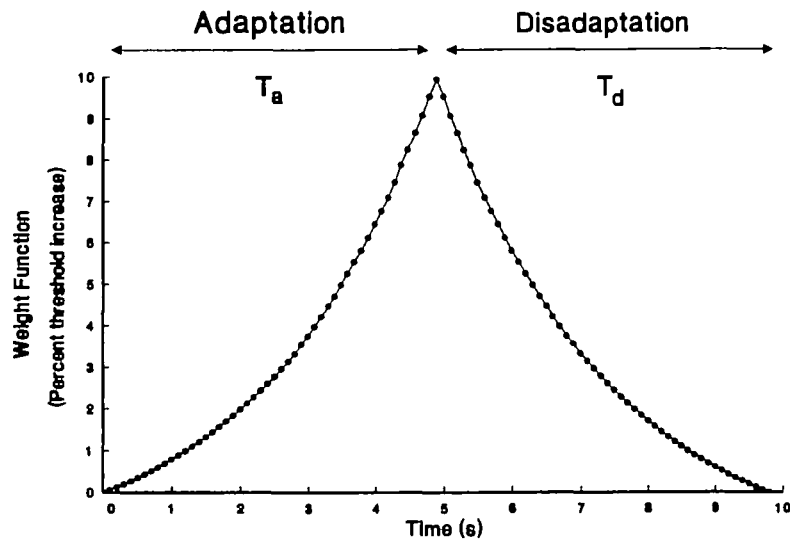


Fig. 1. Diagram showing the W_t used in equations 1 and 2. The percentage threshold increase is shown for example only. The actual value of W_t will depend upon the stimulus profile over the time period considered. X-axis is time since a particular stimulus was sampled by a cell.

W_{ad} depending on the value of t . The number of model cell types with different values of T_a and T_d is virtually infinite. Therefore, for the sake of simplicity, five model cells with large differences in time constants were developed. For this study, T_a and T_d had the values 0.5, 1, 2, 5 and 10 s. Although they could vary independently, T_a and T_d were kept identical for the five model cells presented here. Thus, model cell properties ranged from very rapid model cells ($T_a = T_d = 0.5$ s) to very slow model cells ($T_a = T_d = 10$ s).

Studies have demonstrated that detection of an odor occurs only at stimulus concentrations above the adapted threshold (Borroni and Atema, 1988; Todrank *et al.*, 1991). Thus, the response of the model receptor cell can be modeled by a simple logarithmic dose–response function based on the stimulus concentration above threshold. The response of the model cell is given by equation 4:

$$R_c = B \times \log (C_t - R_t) + A \quad (4)$$

where A is the spontaneous activity of the model cell (in spikes/100 ms), B is the change in spikes per log step change in concentration. B was chosen to be 6 spikes per log change per 200 ms and A was set to zero. The value for B was chosen to be in the mid to low range from published studies (5–25 spikes per 200 ms peak response in insects: Kaissling, 1985; Bartell and Rumbo, 1985; 3–14 spikes per 200 ms in lobsters: Borroni and Atema, 1988; Johnson *et al.*, 1991). The absolute value of B has little bearing on the qualitative outcome of the model, larger values will only serve to enhance differences in response activity. Thus, a conservative value was chosen. The spontaneous activity was set to zero for simplicity. Receptor populations from different species will have different spontaneous activities. The effect of spontaneous activity on the results of the model will be dealt with in the discussion.

To determine the temporal response properties of the model cells, they were presented with three different test stimuli: 1 mM stimulus for 20 s, 1 mM stimulus for 20 s followed by 1 s of 1 mM (stimuli were separated by 1 s of zero background), and three different ramps with a final concentration of 0.2 mM.

Data and signal analysis

Spectral analysis of odor profiles and model cell responses were calculated by a fast Fourier Transform method using a commercial signal processing program (DADiSP Worksheet). Fourier analyses were performed on chemical signals and the responses of the model receptor cells that have been divided into 20-s time bins. The 20-s spectral profiles were subsequently averaged for each signal and this average was used as the best estimate of the true frequency spectrum. [Although this results in a loss of frequency resolution, it also reduces the bias in the estimate (D. Mountain, personal communication).] Fourier analysis reduces a complex wave form into its component pure sine waves with different frequencies and amplitudes. This type of analysis produces a ‘power versus frequency’ plot, where frequency is expressed as cycles per second (as in a pure sine wave). In electrical terms, power is the integral of the root mean square of the voltage over a given frequency range. Here, power reflects the pulse concentration (of the chemical signal) or number of spikes (model cell response) at a particular data point. Again, in electrical terms, frequency is the inverse of the period of the different component sine waves of the signal being analysed. In chemical terms,

onset slopes (chemical signal) or frequency of response (model cell response) is represented as frequencies: a steep slope with a short rise time is expressed in high frequency components. Spectral analysis of an odor profile shows the mean value of pulse amplitudes within each frequency band, while the spectral analysis of the model cell's response will provide insight into which odor frequencies are enhanced or filtered. To further enhance the graphical representation of the enhancement or filtering of frequencies, the spectrum from the odor signal was subtracted from the spectrum of the model cell output. This procedure results in a plot where values above zero indicate enhancement and values below zero indicate filtering of the odor signal. While the frequency analyses itself is independent of the order of presentation of odor pulses, the responses of adapting and disadapting model cells are not. Since the frequency analysis of the model cell responses is based on the output of the model, they become highly indicative of the temporal nature of pulse trains present in the chemical signal and the time constants used for the rates of adaptation and disadaptation.

Environmental stimulus profiles

The stimulus profiles that served as the inputs for the model cells were recorded in a flow-through flume (250×90×20 cm) under conditions in which lobsters, *Homarus americanus* showed orientated movements toward the odor sources. (Details on the flow set-up and recording parameters are in Moore and Atema, 1991b.) Recordings were made at 10 Hz using the IVEC-5 (In Vivo Electrochemistry Computer System; Medical Systems Corp.) and microelectrochemical electrodes (diameter 150 μ). Three samples (3 min each) recorded 25, 50 and 100 cm from the odor source were used in this study. Further details of recording and digitizing are explained elsewhere (Moore *et al.*, 1991b).

Results

When presented with a 1 log step increase in stimulus concentration for 20 s (Figure 2A), the model cells responded and then adapted according to their individual time courses (Figure 2). The rapidly adapting model cells (Figure 2B and C) gave robust responses only during the initial portion of the stimulation. After this, they quickly adapted and did not respond. Conversely, the slowly adapting model cell (Figure 2F) responded for over half of the stimulation period before adapting. When presented with a 1-s pulse of stimulus after the 20-s pulse ended (Figure 3A), the model cells again responded, showing disadaptation according to their time constants. The rapidly disadapting model cells (Figure 3B and C) responded to both pulses, although the 1 s model cell responded less to the second pulse than it did to the first pulse. The slowly disadapting model cells (Figure 3E and F) were still adapted to the 20-s pulse and did not respond to the following 1-s pulse.

Model cells presented with stimulus ramps each reaching the same final concentration, but at differing rates of change in concentration, responded according to their adaptation and disadaptation time courses. The rapidly adapting model cell (Figure 4B) responded briefly to the fastest ramp, but did not respond to the slower two ramps because it adapted to the stimulus concentration before it rose above its threshold. The model cells with time constants of 1 and 2 s responded to the two faster ramps, but not to the slowest ramp (Figures 4C and D). Conversely, the slow model cells (5- and 10-s time constants) responded to all three ramps, but displayed a greater response (as

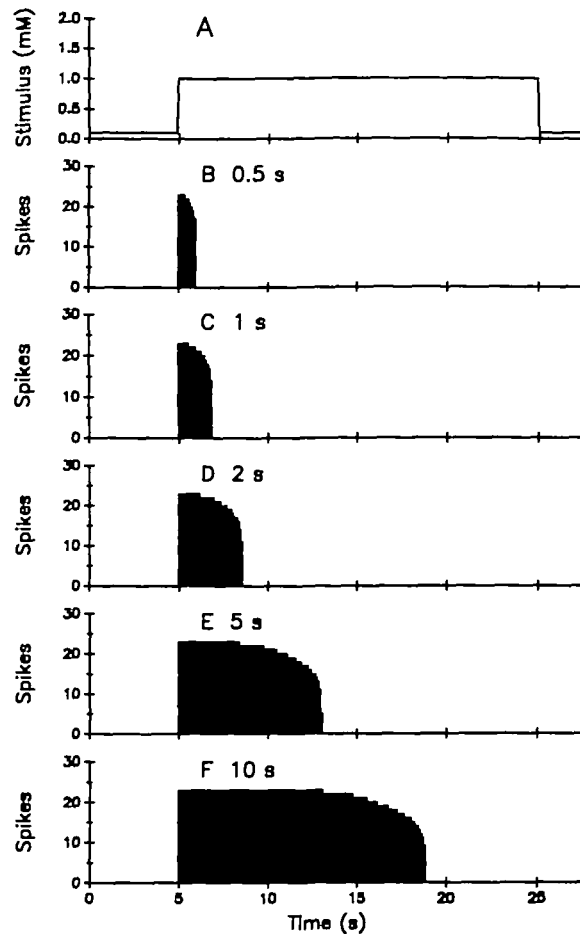


Fig. 2. (A) A 1 log-step 20-s square pulse presented to five different model receptor cells. (B–F) Response histograms of the five model cells to stimulus in (A). Numbers above each graph represent adaptation and disadaptation time courses. Y-axis is mM for stimulus profile and spikes per 100 ms for receptor cells. Time courses are 0.5 (B), 1 (C), 2 (D), 5 (E), 10 (F) s for both adaptation and disadaptation. Order of the presentation of receptor output will remain consistent in subsequent figures.

in number of spikes per bin) to the fastest ramp (Figure 4E and F).

Naturally occurring odor signals are characterized by large fluctuations in intensity, including periods of little to no concentration (Figures 5A and 7A). These fluctuations change in intensity and frequency with increasing distance from the odor source. Figure 5A shows a 1-min record from a turbulent odor plume. Figure 5B–F show the spike trains from the five model receptor cells stimulated with the signal in Figure 5A. The response from the rapidly adapting model cell (Figure 5B) was characterized by short, intermittent bursts that occur at nearly every odor pulse. In contrast, the response from the slowly adapting model cell (Figure 5F) was characterized by longer lasting periods of bursts that either combined responses to many odor pulses into one spike train or missed them altogether. A particularly clear example of the differences in responses from the model cells is shown between 28 and 33 s (Figure 5). The 0.5 s

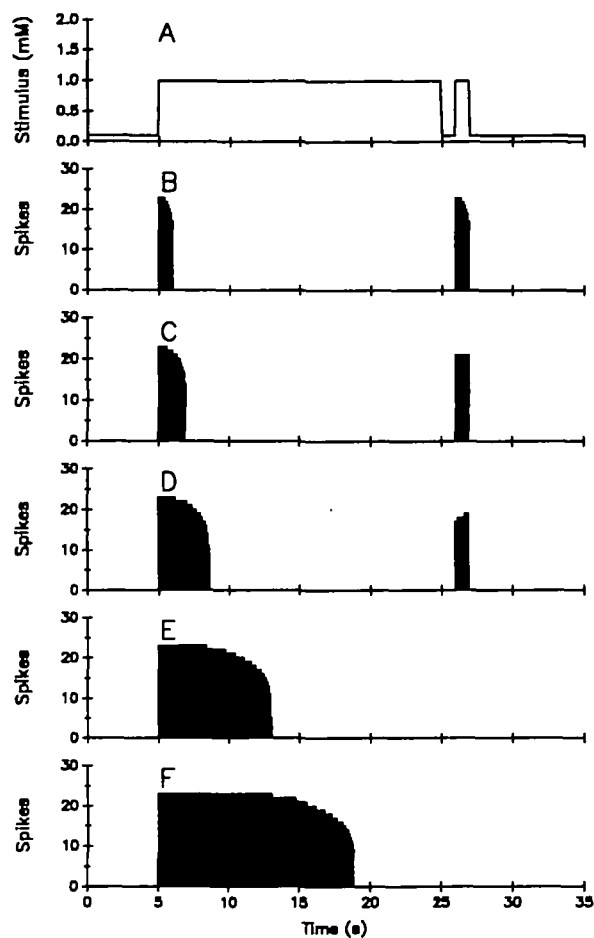


Fig. 3. (A) A 1 log-step 20-s square pulse followed by a 1 log-step 1 second square pulse. Time between stimulus presentations is 1 second. (B–F) Response histograms of the five model cells to stimulus in (A). Numbers above each graph represent adaptation and disadaptation time courses. Y-axis is mM for stimulus profile and spikes per 100 ms for receptor cells.

model cell encoded the stimulus profile as five distinct pulses. The 1-s model cell encoded this as three pulses, while the 2-s model cell perceived only one pulse. The 5-s model cell encoded two pulses and the 10-s model cell did not fire.

Frequency spectra of both the odor signal and model cell output can be used to analyse how the inherent frequencies within an odor signal are enhanced or filtered by the model cell properties. Figure 6A shows a frequency spectrum of the odor signal recorded 25 cm from the odor source (Figure 5A). Figure 6B–F shows the difference between the frequency spectra from spike trains from the model cells (Figure 5B–F) and the odor signal (Figure 5A). This was calculated by simply subtracting the frequency spectrum from the odor signal from the frequency spectrum of the model cell output. Thus, a positive value indicates that part of the spectrum that was enhanced by the model cell and a negative value shows that part of the spectrum that was filtered by the model

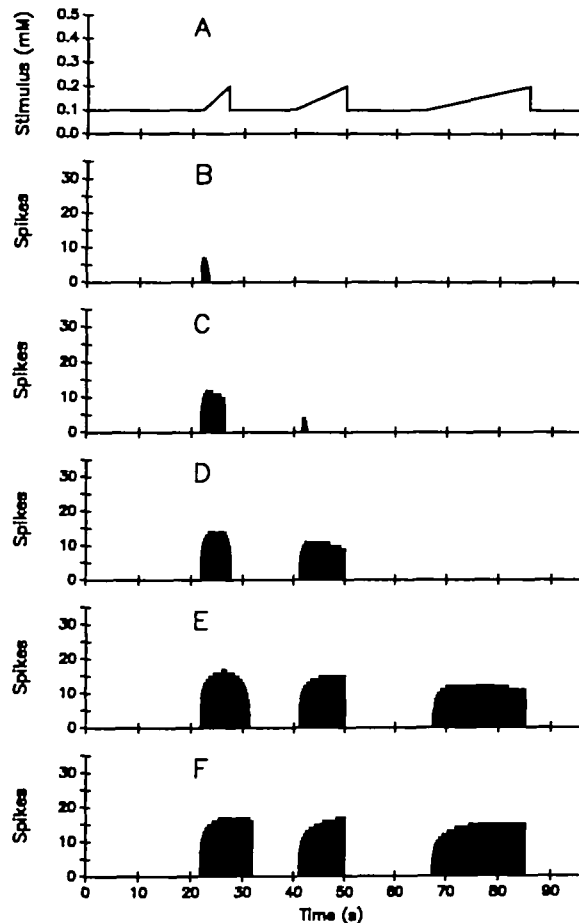


Fig. 4. (A) Stimulus profile of 0.1 log (final concentration) ramps presented to the five model receptor cells. (B–F) Response histograms of the five model cells to the ramp stimuli (A). Ramps were presented separately, but are shown together for simplicity. Ramps have the same final concentration but different rates of increase (slope). Slopes are 20, 10 and 5 micromolar/s, respectively.

cell. These spectra show that each model cell enhanced a different component of the frequency spectrum, acting as a ‘band pass’. For this particular odor signal, the fast adapting and disadapting model cell enhanced that part of the odor signal that has frequency components at 0.4–0.5 and 0.6–0.7 Hz (compare Figure 6A and 6B). This model cell also filtered out those frequency components that occur below 0.2 Hz. This part of the odor signal (0.4–0.5 Hz) was also enhanced in the 1 and 2 s model cells (Figure 6C and 6D), but to a lesser degree than the faster adapting model cell. Conversely, the frequency component that was only slightly enhanced by the fast model cell (0.2 Hz; Figure 6B) was greatly enhanced by the slower model cells reaching a maximum at the 2-s model cell (Figure 6D). The lowest frequencies (>0.2 Hz) were enhanced the greatest by the slowest adapting model cells (Figure 6E and F) and were almost completely filtered by the rapidly adapting model cells (Figure 6B, 6C and 6D).

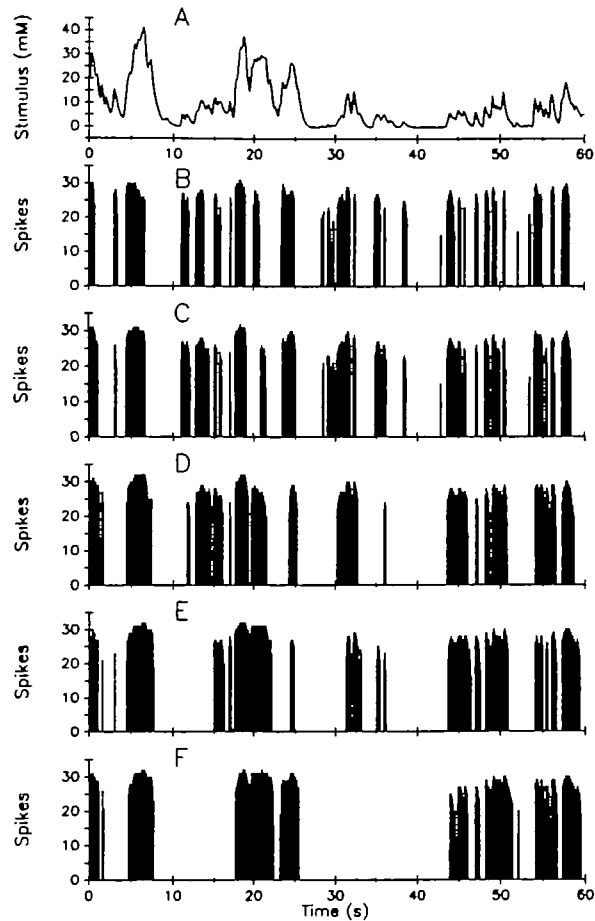


Fig. 5. (A) Stimulus profile of a turbulent odor plume recorded 25 cm from the source. (B–F) Temporal response pattern of model receptor cells with different time courses of adaptation/disadaptation.

These model cells were functionally similar to a band pass filter. The fast adapting model cells were selectively enhancing a frequency range from 0.4 to 0.7 Hz and filtering out lower frequencies, while the slower model cells had their band pass filters set to a lower range of frequencies (<0.4 Hz).

As odor signals travel farther from the odor source, the intensity fluctuations become less intense and spaced farther apart (compare Figure 7A with Figure 5A). The pattern of responses in Figure 5 is also seen in Figure 7. The 0.5 s model cell responses were mainly short bursts (Figure 7B), while the 10-s model cell responses occurred in longer spike trains. This pattern is not, however, always observed. For example, the stimulus profile from 0 to 10 s (Figure 7A) was encoded as five discrete pulses by the rapid model cell (Figure 7B: 0–10 s) and as one pulse by the slow model cell (Figure 7F: 0–10 s). Conversely, the stimulus profile from 41 to 43 s was encoded as one pulse by the rapid model cell (Figure 7B: 41–43 s), one very short pulse by the 5 s model cell (Figure 7C: 41–43 s) and two pulses by the 10-s model cell (Figure 7F: 41–43 s).

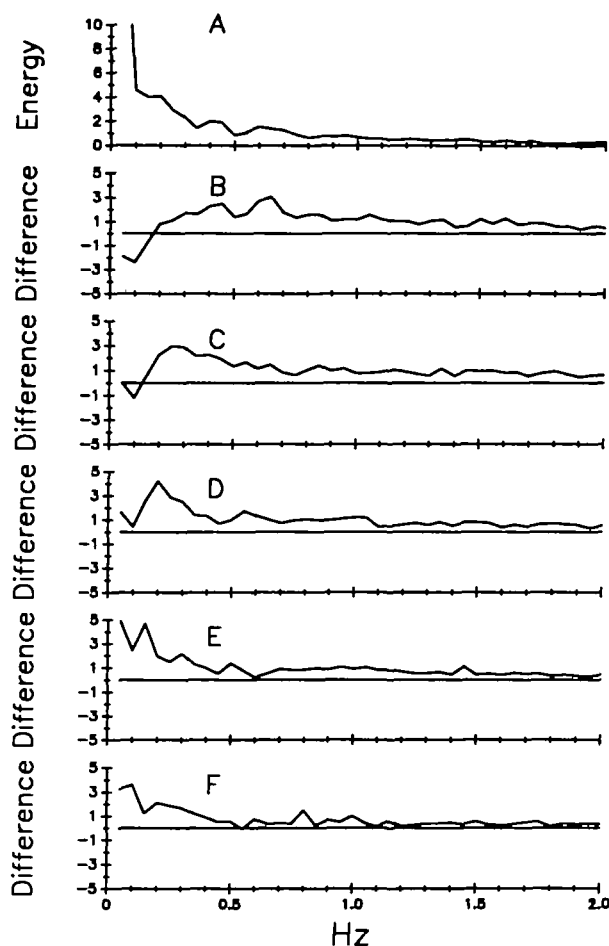


Fig. 6. Frequency spectra of a turbulent odor signal recorded 25 cm from a source (A) and of the difference frequency spectrum of the responses of the five model cells to the odor signal (B–F). Ordinate for (A) is expressed as energy which corresponds to the number and strength of responses (or pulses and pulse amplitude for odor signal; See text for detailed explanation). Ordinate for (B–F) are the values for the differences between the model cell output and the odor plume spectrum. A positive value means that part of the spectrum is enhanced by the model cell, whereas a negative value means that the spectrum is filtered.

Discussion

The strength of any physiological model lies in its ability to predict the responses of real cells to known stimuli and provide insight into questions not readily solved by physiological techniques. In this way, models point out gaps in knowledge about a particular system and serve to guide further research. The model chemoreceptor cells in this study have temporal firing properties similar to those found in real chemoreceptor cells (Borroni and Atema, 1988; Voigt and Atema, 1990; Kaissling *et al.*, 1987). The model cells stop firing when presented with a prolonged stimulus (Figure 2) and the rate at which the model cells stop firing is dependent upon the adaptation time course for each model cell. Model cells with rapid time courses respond and then quickly adapt

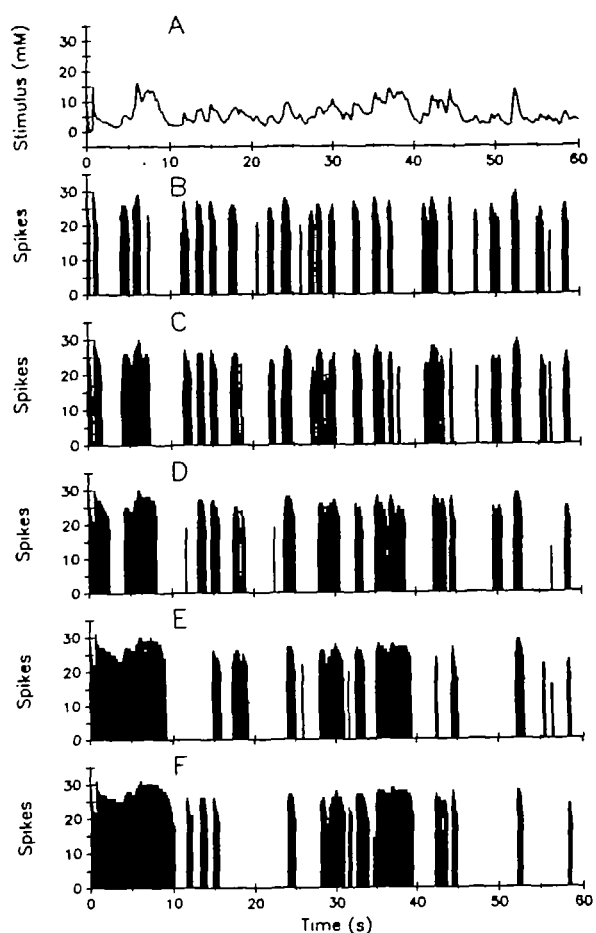


Fig. 7. (A) Stimulus profile of a turbulent odor plume recorded 50 cm from the source. (B–F) Temporal response pattern of model receptor cells with different time courses of adaptation/disadaptation.

to prolonged stimulation (Figure 2A and B). In contrast, model cells with slow time courses respond for a relatively long time before adapting (Figure 2E and F). The rate at which the model cells disadapted was also consistent with their different time courses. The slowly disadapting model cells did not respond to short pulses presented 1 s after the adapting pulse (Figure 3E and F), while the rapidly disadapting model cells did respond to the short pulse (Figure 3B and C). These properties make receptor cells sensitive to both the absolute concentration and rate of change in concentration (Figure 4).

When presented with realistic odor profiles, model cells respond to the current (adapting) concentration ($t = 0$) in a manner that is dependent upon the past stimulation patterns. This results in a model cell output that is not only dependent on the current concentration but also past concentrations and the order in which they arrived at the model cell. For example, compare the responses from the slow adapting model cell

to the stimulus profile between 32–34 and 48–51 s (Figure 5A and F). The stimulus profiles are very similar to double peaks of concentrations around 15 mM. Because of the dynamic adaptation state of the model cell, it does not respond to the first stimulus, yet gives a robust response to the second profile. Thus, for any cell the most stimulatory profiles, such as concentration level, rate of increase of concentration, or frequency of stimulation pulses, will be determined by its adaptation and disadaptation properties.

In addition, this study shows that by having temporally dynamic response properties, model receptor cells become analogs to ‘band-pass’ filters, selectively allowing certain frequencies of signal fluctuations through and filtering out all other frequencies (Figure 6). Unlike true band-pass filters, which are only dependent on the frequency and not the amplitude of the input signal, the filtering performed by the model cells in this study is dependent on both the amplitude and frequency of the odor pulses. This means that the actual frequencies that are ‘passed’ by real receptor cells may change over time due to interactions between concentration fluctuations in odor signals and adaptation differences in receptors cells.

It has been suggested that the temporal filter properties chemoreceptor cells are matched to the dominant frequencies within biologically relevant turbulence (Atema, 1988; Moore and Atema, 1988). The dominant frequencies in aquatic odor plumes that have been quantified are below 4 Hz (Moore and Atema, 1991; Moore *et al.*, 1994). The time constants used in this study, which were taken from physiological experiments, appear to filter and enhance those portions of the odor signals that are most dominant within biologically relevant odor plumes, although, some higher frequencies (2–4 Hz) were essentially unchanged by the model receptor cells.

Studies on odor plumes in air have shown them to be quite similar to the types of signals seen in aquatic situations (Murlis and Jones, 1981; Murlis *et al.*, 1991). Terrestrial odor signals are also quite heterogeneous with large fluctuations in concentration, but the signals within the odor ‘bursts’ appear to rise much faster than aquatic odor signals. Also, the ‘bursts’ themselves seem to be spaced further apart in time with respect to aquatic odor signals. If these general differences hold true then terrestrial receptor cells should have faster rates of adaptation and disadaptation. The ability of some insect neurons to resolve 10 Hz fluctuations (Kaissling *et al.*, 1987; Christensen and Hildebrand, 1988; Rumbo and Kaissling, 1989), while the fastest frequency resolution shown for any aquatic system is around 4 Hz (Gomez *et al.*, 1992), is consistent with this hypothesis. (Frequency analysis of terrestrial odor signals has not been published, so a direct comparison of the temporal aspects of aquatic and terrestrial signals cannot be made.) In the future, it may be possible to apply this model to turbulent odor signals from terrestrial environments.

Besides the fluctuating odor signal within turbulent odor plumes, many animals actively sample the odor signal by rapidly changing fluid motions, which will alter the local concentration fluctuations. Crustaceans sample odor signals by flicking their antennules; lobsters only flick their lateral filament and not their medial filament. Catfish will periodically flick their barbels rapidly. Vertebrates (aquatic and terrestrial) will sniff which increases the fluid velocities in the nasal cavity. The intense mixing that occurs during these behavior patterns may eliminate the small scale fluctuations of the odor signal leaving only large changes in intensity (Moore *et al.*, 1991a,b). Conversely, thick boundary layers surrounding non-sampling appendages serve to filter out high frequency

components of odor signals. Differences in sampling behavior of chemosensory appendages will add yet another level of complexity to the temporal filtering discussed in this paper.

In this study, the model receptor cells had identical adaptation and disadaptation time constants. Adaptation and disadaptation have two separate effects on the temporal filtering capabilities of receptor cells. The rate of adaptation determines which slopes (rate of increase of concentration) are most stimulatory for a model cell (Figure 4). Rapidly adapting model cells do not respond to slow changes in concentration and need more rapid changes to overcome the rapid rate of adaptation (Figure 4B, C and D). Slowly adapting model cells detect very little difference in the more rapid changes in concentration and do not respond at all to very slow increases (Figure 4E and F).

In contrast, the rate of disadaptation (recovery from adaptation) determines the frequency of stimulation (pulse rate) that a model cell can resolve. Rapidly disadapting model cells can resolve faster pulse frequencies than slowly disadapting model cells (compare Figure 7B with 7F, 0–10 s). These model cells respond only briefly, but can follow high frequency stimulus pulses. Slowly disadapting model cells respond for much longer periods of time, but frequently do not resolve short odor pulses. Thus, although adaptation and disadaptation contribute to different aspects of filtering, the overall temporal filter properties of receptor cells are determined by the interaction of these two processes.

Previous physiological studies with invertebrates (Zack-Strausfeld and Kaissling, 1986; Borroni and Atema, 1988; Voigt and Atema, 1990; Borroni and O'Connell, 1992), behavioral studies in humans (Cain, 1970; Berglund *et al.*, 1971; Todrank *et al.*, 1991) and the model receptor cells in this study show that changes in receptor cell threshold, resulting from adaptation and disadaptation, will alter the response of a cell to a particular concentration. This change will depend upon the previous odor profile (and response to it) presented to the receptor cell. For example, the slowest adapting model cell does not respond to pulses ranging from 8 to 15 micromolar at one point in time (Figure 5; 10–15 s), but in the same profile elicits robust responses at the same stimulus concentration (Figure 5, 43–46 s). Although these stimuli are roughly equal in concentration, the model cell does not respond to the first pulse due to a large adapting stimulus before the odor pulse (Figure 5, 5–8 s). There is no adapting pulse before the second pulse, so the model cell gives a full response to the odor.

Changes in the response properties of receptor cells in turbulent odor plumes are important in considering how information is extracted from natural signals, in particular the encoding of intensity information. Many intensity coding schemes have been postulated in recent years. These schemes, based on receptor cell responses to static stimuli in physiological recording chambers, have centered on the coding of stimulus intensity by across-fiber patterns (Johnson *et al.*, 1987, 1991) or mass-responses by receptor cell populations (Ganchrow and Erickson, 1970; Girardot and Derby, 1988; Derby *et al.*, 1991).

These coding models have been developed from non-adapted neural responses to static stimulus presentations. Consequently, although they provide some insight into the coding of environmental intensity patterns, they may not accurately reflect the intensity responses of receptor cells under environmentally realistic odor stimulation. For any model to

work under turbulent signal conditions and the subsequent changes in receptor responses, it must either be robust enough to withstand large changes in dose–response functions or plastic enough to encode differences in intensity during adaptation at the peripheral receptor cells. It remains to be seen if these schemes can incorporate both adaptation and temporally dynamic stimulus profiles and still maintain the same predictions.

The model presented in this paper, with additional data from physiological studies, can be used to study how chemoreceptor cells filter environmental information contained in odor signals and encode specific features such as temporal frequency and odor intensity. This study has shown that adaptation and disadaptation properties of receptor cells determine which stimulus profiles will elicit the largest responses. Adaptation and disadaptation selectively enhance some frequencies in odor signals and filter out others. The frequencies that are enhanced or filtered are determined by the interaction between frequencies and amplitudes within odor plumes and the time constants of receptor cells. Any coding scheme must incorporate the dynamic response capabilities of receptor cells to accurately reflect receptor responses under biologically relevant stimulation.

Acknowledgements

This work is supported by an ADMH Drug Training Fellowship (AA07464) to PM. and by the Kirin Brewery Co., Ltd. The author would like to thank Drs Thomas Christensen, Jelle Atema and Rainier Voigt for valuable discussion on the ideas presented here, Drs John Teeter and Bruce Bryant for detailed and helpful comments on the manuscript, and an anonymous reviewer for critical suggestions.

References

- Almaas, T.J., Christensen, T.A. and Mustaparta, H. (1991) Chemical communication in heliothine moths I. Antennal receptor neurons encode several features of intra- and interspecific odorants in the male corn earworm moth *Helicoverpa zea*. *J. Comp. Physiol. A.*, **169**, 249–258.
- Atema, J. (1988) Distribution of chemical stimuli. In Atema, J., Popper, A.N., Fay, R.R. and Travolgo, W.N. (eds), *Sensory Biology of Aquatic Animals*. Springer-Verlag, NY, pp. 29–56.
- Bartell, R.J. and Rumbo, E.R. (1985). Correlations between electrophysiological and behavioral responses elicited by pheromone. In Payne, T.L., Birch, M.C. and Kennedy, C.E.J. (eds), *Mechanisms in Insect Olfaction*. Clarendon Press, Oxford, pp. 169–174.
- Baylin, F. and Moulton, D.G. (1979) Adaptation and cross-adaptation to odor stimulation of olfactory receptors in the tiger salamander. *J. Gen. Physiol.*, **74**, 37–55.
- Bell, W.J. and Tobin, T.R. (1982) Chemo-orientation. *Biol. Rev.*, **57**, 219–260.
- Berglund, B., Berglund, U., Engen, T. and Lindvall, T. (1971) The effect of adaptation on odor detection. *Percept. Psychophys.*, **9**, 435–438.
- Borroni, P. and Atema, J. (1988) Adaptation in chemoreceptor cells: I. Self-adapting backgrounds determine threshold and cause parallel shifts of response function. *J. Comp. Physiol. A.*, **164**, 67–74.
- Borroni, P.F. and O'Connell, R.J. (1992) Temporal analysis of adaptation in Moth, *Trichoplusia ni* pheromone receptor neurons. *J. Comp. Physiol. A.*, **170**, 169–700.
- Cain, W.S. (1970) Odor intensity after self- and cross-adaptation. *Percept. Psychophys.*, **7**, 271–275.
- Cain, W.S. (1977a) Differential sensitivity for smell: 'noise' at the nose. *Science*, **195**, 796–798.
- Cain, W.S. (1977b) Odor magnitude: coarse vs fine grain. *Percept. Psychophys.*, **22**, 545–549.
- Cardé, R.T., Dindonis, L.L., Agar, B. and Foss, J. (1984) Apparency of pulsed and continuous pheromone to male gypsy moths. *J. Chem. Ecol.*, **10**, 355–348.
- Christensen, T.A. and Hildebrand, J.G. (1988) Frequency coding by central olfactory neurons in the sphinx moth *Manduca sexta*. *Chem. Senses*, **13**, 123–130.
- Derby, C.D., Girardot, M.-N. and Daniel, P.C. (1991) Responses of olfactory receptor cells of spiny lobsters to binary mixtures. I. Intensity mixture interactions. *J. Neurophysiol.*, **66**, 112–130.

- Ganchrow, J.R. and Erickson, R.P. (1970) Neural correlates of gustatory intensity and quality. *J. Neurophysiol.*, **33**, 768–783.
- Girardot, M.-N. and Derby, C.D. (1988) Neural coding of quality of complex olfactory stimuli in lobsters. *J. Neurophysiol.*, **60**, 303–324.
- Gomez, G., Voigt, R. and Atema, J. (1992) Frequency coding in chemoreceptor cells. *Chem. Senses*, **17**, 631–632.
- Hodgson, E.S. and Mathewson, R.F. (1971) Chemosensory orientation in sharks. *Ann. NY Acad. Sci.*, **188**, 175–182.
- Johnsen, P.B. and Teeter, J.H. (1980) Spatial gradient detection of chemical cues by catfish. *J. Comp. Physiol. A.*, **140**, 95–99.
- Johnson, B.R., Voigt, R., Merrill, C. and Atema, J. (1987) Stimulus intensity discrimination by lobster olfactory receptors. *Chem. Senses*, **12**, 668.
- Johnson, B.R., Voigt, R., Merrill, C. and Atema, J. (1991) Across-fiber patterns may contain a sensory code for stimulus intensity. *Brain Res. Bull.*, **26**, 327–331.
- Kaissling, K.-E. (1985) Temporal characteristics of pheromone receptor cell responses in relation to orientation behavior of moths. In Payne, T.L., Birch, M.C. and Kennedy, C.E.J. (eds), *Mechanisms in Insect Olfaction*. Clarendon Press, Oxford, pp. 193–199.
- Kaissling, K.E., Zack-Straussfeld, C. and Rumbo, E. (1987) Adaptation processes in insect olfactory receptors: mechanisms and behavioral significance. In Roper, S. and Atema, J. (eds), *Olfaction and Taste IX*. *N.Y. Acad. Sci.*, **510**, 104–112.
- Kennedy, J.S. (1986) Some current issues in orientation to odour sources. In: Payne, T.L., Birch, M.C. and Kennedy, C.E.J. (eds), *Mechanisms in Insect Olfaction*. Clarendon Press, NJ, pp. 11–25.
- McBurney, D.H., Kasschau, R.A. and Bogart, L.M. (1967) The effect of adaptation on taste judgments. *Percept. Psychophys.*, **2**, 175–178.
- Michel, W.C. and Ache, B.W. (1991) Odor-activated K⁺-conductance inhibits lobster olfactory receptor cells. *Chem. Senses*, **15**, 619–620.
- Moore, P.A. and Atema, J. (1988) A model of a temporal filter in chemoreception to extract directional information from a turbulent odor plume. *Biol. Bull.*, **174**, 355–363.
- Moore, P.A. and Atema, J. (1991) Spatial information in the three-dimensional fine structure of an aquatic odor plume. *Biol. Bull.*, **181**, 408–418.
- Moore, P.A., Scholz, N. and Atema, J. (1991a) Chemo-orientation of lobsters, *Homarus americanus* in turbulent odor plumes. *J. Chem. Ecol.*, **17**, 1293–1307.
- Moore, P.A., Atema, J. and Gerhardt, G.A. (1991b) Fluid dynamics and microscale odor movement in the chemosensory appendages of the lobster, *Homarus americanus*. *Chem. Senses*, **16**, 663–674.
- Moore, P.A., Weissburg, M.J., Parrish, J.M., Zimmer-Faust, R.K. and Gerhardt, G.A. (1994) Spatial distribution of odors in simulated benthic boundary layer flows. *J. Chem. Ecol.*, **20**, 255–279.
- Murlis, J. and Jones, C.D. (1981) Fine-scale structure of odour plumes in relation to insect orientation to distant pheromone and other attractant sources. *Physiol. Entomol.*, **6**, 71–86.
- Murlis, J., Willis, M.A. and Cardé, R.T. (1991) Odour signals: patterns in space and time. In Døving, K. (ed.), *Proceedings of the Tenth International Symposium on Olfaction and Taste Graphic Communication System*, Oslo, pp. 6–17.
- Rumbo, E.R. and Kaissling, K.-E. (1989) Temporal resolution of odor pulses by three types of pheromone receptor cells in *Antheraea polyphemus*. *J. Comp. Physiol. A.*, **165**, 281–291.
- Todrank, J., Wysocki, C.J. and Beauchamp, G.K. (1991) The effects of adaptation on the perception of similar and dissimilar odors. *Chem. Senses*, **16**, 467–482.
- Voigt, R. and Atema, J. (1990) Adaptation in chemoreceptor cells. III. Effects of cumulative adaptation. *J. Comp. Physiol. A.*, **166**, 865–874.
- Weber, E.H. (1978) *E.H. Weber: the Sense of Touch*. Ross, H.E. and Murray, D.J. (trans.) Academic Press, New York.
- Zack-Straussfeld, C. and Kaissling, K.-E. (1986) Localized adaptation processes in olfactory sensilla of Saturniid moths. *Chem. Senses*, **11**, 499–512.
- Zimmer-Faust, R.K. (1991) Chemical signal-to-noise detection by spiny lobsters. *Biol. Bull.*, **181**, 419–426.

Received on August 3, 1993; accepted on November 18, 1993